

Sensitivity and spatial specificity of multiple phase-cycled pass-band bSSFP fMRI at 9.4T

S.-H. Park^{1,2}, T. Kim¹, P. Wang¹, T. Q. Duong², and S.-G. Kim¹

¹Radiology, University of Pittsburgh, Pittsburgh, PA, United States, ²Research Imaging Institute, Ophthalmology/Radiology, University of Texas Health Science Center at San Antonio, San Antonio, TX, United States

Introduction

Pass-band bSSFP is a promising tool for high-resolution fMRI, but its signal sources have been unclear because there are two distinctive frequency bands, i.e., phase-insensitive pass bands and phase-sensitive transition bands. Understanding the signal sources of bSSFP fMRI is important because different signal sources (T_2 or T_2^*) yield differential sensitivity and spatial specificity, as observed in fMRI studies with spin-echo and gradient-echo EPI techniques (1). In previous studies, characteristics of pass-band bSSFP fMRI has been reported as T_2^* at long TR and T_2 at short TR (2,3). Since activation pixels have different mixtures of tissue, microvasculature, and draining veins, the contribution of T_2 and T_2^* to bSSFP fMRI varies, depending on the spatial regions and shimming conditions. In this study, we investigated the spatial heterogeneity in characteristics of high resolution bSSFP fMRI signal at multiple phase cycling angles. Changes in sensitivity and spatial specificity of bSSFP fMRI were assessed at different activation sites as a function of phase cycling angle at two different TR values. The signal characteristics in activation sites were investigated by comparing the fMRI maps with BOLD venogram (4) and baseline transition-band bSSFP images.

Material and Methods

Three male Sprague-Dawley rats weighing 300–450 g were used with approval from the IACUC. The rats were initially anesthetized and then intubated for mechanical ventilation. The femoral artery and femoral vein were catheterized for blood gas sampling and for fluid administration, respectively. After the surgical procedure, isoflurane level was maintained at 1.4%. The head of the animal was carefully secured to a home-built cradle. Rectal temperature was maintained at 37 ± 0.5 °C. Ventilation rate and volume were adjusted based on blood gas analysis results. Electrical stimulation was applied to either the right or left forelimb using two needle electrodes. Stimulation parameters for activation studies were: current = 1.2–1.6 mA, pulse duration = 3 ms, repetition rate = 6 Hz, stimulation duration = 15 s, and inter-stimulation period = 3 min (5).

All experiments were carried out on a Varian 9.4 T / 31-cm MRI system with an actively-shielded gradient coil of 12-cm inner diameter. A homogeneous coil and a surface coil were used for RF excitation and reception, respectively. For fMRI studies, eight pass-band bSSFP and one GRE studies were performed. Four bSSFP studies were performed with TR / TE = 20/10 ms and the remaining four bSSFP studies with TR / TE = 10/5 ms. Each set of four bSSFP studies was composed of four different phase cycling angles of 0°, 90°, 180°, and 270°. The GRE fMRI study was performed with TR / TE = 20/10 ms. The resolution parameters were the same for all the 9 fMRI techniques: matrix size = 256×192 , FOV = 2.4×2.4 cm², number of slice = 1, and slice thickness = 2 mm. Flip angles for all the bSSFP studies and the GRE study were 16° and 8°, respectively, optimized based on simulation (data not shown). Twenty four images were acquired for each fMRI study; eight during prestimulus baseline, four during stimulation, and twelve during the poststimulus period. Resonance frequency was recalibrated before each fMRI study to minimize B_0 drifting effects. The nine fMRI studies with bSSFP and GRE composed one full set and each full set was repeated 15 to 25 times. Eight baseline transition-band bSSFP images were additionally acquired with the scan parameters the same as the corresponding pass-band bSSFP used for fMRI except flip angles of 4° and 2° at TR/TE values of 20/10 ms and 10/5 ms, respectively. BOLD microscopy was performed with a 3D RF-spoiled gradient-echo pulse sequence, as described previously (4), with imaging parameters of TR = 40 ms, TE = 20 ms, matrix size = $256 \times 192 \times 128$, FOV = $2.4 \times 2.4 \times 1.2$ cm³, NEX = 2, and total scan time = 18.4 min.

Results and Discussion

If the spin-echo contrast is dominant in bSSFP fMRI with short TE and TR, then its largest BOLD signal change should be located at the middle of the somatosensory cortex, since the highest metabolic and blood changes occur at layer 4. If the gradient-echo contrast is dominant, the highest BOLD percent change is likely to be located at the surface of the cortex, where large draining veins exist. Hot spots (yellow pixels) in pass-band bSSFP fMRI maps were shifted with different phase cycling angles at the long and short TR/TE conditions (Fig. 1a–h). Activation foci (yellow pixels) were located following three different cortical regions of (i) the cortical surface (e.g. 90° and 180° phase cycling in TR of 10 ms), (ii) the middle cortical regions (mostly 0° and 270° phase cycling), and (iii) intracortical veins (Fig. 2b,c,e). In all the animals tested, we could find a condition that showed minimal correlation with both cortical surface veins and intracortical veins while maintaining high sensitivity to BOLD contrast (Fig. 1d,h). These activation foci in the bSSFP fMRI maps were well correlated with the high intensity regions in baseline transition-band bSSFP images (Fig. 1i–p), where high intensity and low intensity regions represent steep and flat phase changes, respectively.

This result implies that steep phase changes in transition bands are dominating factor over baseline intensity for pass-band bSSFP fMRI at high field. The insensitiveness of pass-band bSSFP fMRI to baseline intensity implies its insensitiveness to B_1 inhomogeneity, in favor of fMRI at high field. Furthermore, because of reduced T_2 / T_1 ratio at high field, the optimal flip angle for pass-band bSSFP can be significantly reduced (~16° at 9.4T vs ~40° at 1.5T), which is also in favor of imaging at high field for reduced specific absorption rate.

In conclusion, we found that bSSFP fMRI signal exhibits spatial heterogeneity depending on many imaging parameters, phase cycling angles, TR, and TE. Large signal change pixels (center of the activation foci) can be modulated by changing phase cycling angle, and can be predicted from transition-band bSSFP signal intensity.

References

1. Zhao et al, Magn Reson Med 51:518-524 (2004).
2. Zhong et al, Magn Reson Med 57:67-73 (2007).
3. Miller et al, Neuroimage 37:1227-1236 (2007).
4. Park et al, Magn Reson Med 59:855-865 (2008).
5. Kim et al, J Cereb Blood Flow Metab 27:1235-1247 (2007).

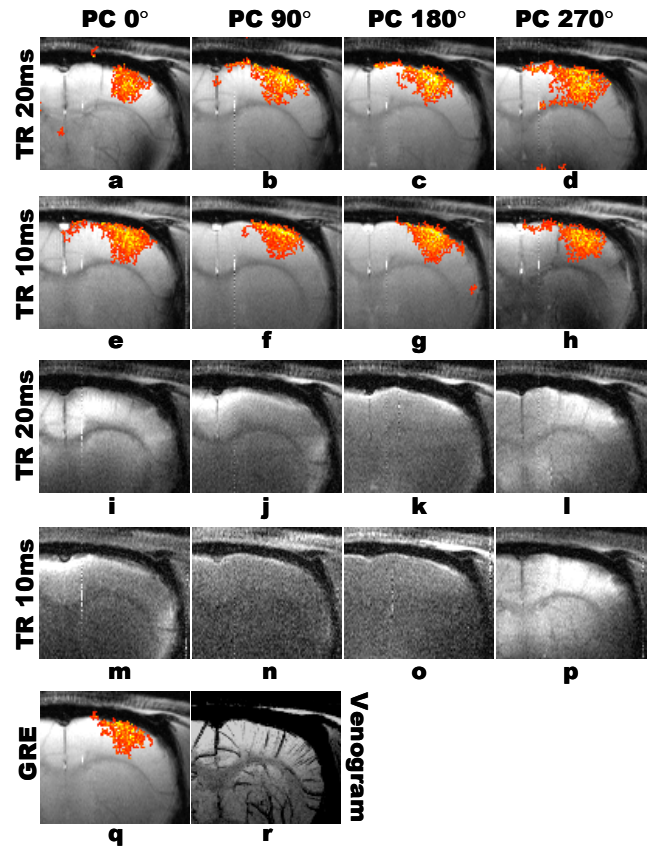


FIG. 1. fMRI maps (a-h,q), baseline transition-band bSSFP images (i-p), and venogram (r). Phase cycling angle and TR values used are described on top and left-hand side of the images.